Contents lists available at GrowingScience

Current Chemistry Letters

homepage: www.GrowingScience.com

Synthesis, characterization and biological activities of NiO-cellulose nanocomposite

Anshu Tamta[a*], Rajesh Kumar[a], Vinita Gouri[b], Rajendra Joshi[a], Bhuwan Chandra[a] and Narain Datt Kandpal[a]

[a]*Department of Chemistry, Kumaun University Nainital, S.S.J. Campus, Almora-263601, Uttarakhand, India*
[b]*Department of Zoology, Kumaun University Nainital, S.S.J. Campus, Almora-263601, Uttarakhand, India*

C H R O N I C L E

Article history:
Received October 28, 2023
Received in revised form
January 3, 2024
Accepted February 2, 2024
Available online
February 2, 2024

Keywords:
Nanocomposite
Cellulose
Biological activities
Antibacterial
Antileishmanial

A B S T R A C T

NiO cellulose nanocomposite (NiO-CN) were synthesized by the precipitation method and characterized by X-Ray diffraction (XRD), Transmission Electron Microscope (TEM), Scanning Electron Microscope (SEM), Energy Dispersive X-ray (EDX) analysis, Fourier transform infrared (FTIR) measurements and UV–vis spectroscopy. The particles obtained have an average size of 20-30 nm as shown by TEM analysis. Fourier transform infrared (FTIR) measurements were carried out to identify the possible biomolecules responsible for the capping and stabilization of the nickel oxide nanoparticles synthesized by milk. The presence of elements in the nanoparticles was also analysed by Energy Dispersive X-ray (EDX) analysis. The results of EDX analysis show the weight percentages of C, O, Ni, and N-elements in the synthesized material were 41.65%, 52.49%, 3.81%, and 2.06%, respectively. Scanning Electron Microscope (SEM) has been used to assess the morphology of the nanoparticle. The effects of NiO-cellulose nanocomposite are screened for biological activities like, antibacterial activity was done by the Disc diffusion method. The bacterial organisms used in this study were *Bacillus subtilis, Salmonela abony, Staphylococcus aureus* and *Escherichia coli*. The observed inhibition zone for these microorganisms was found to be a minimum of 3.0 mm and a maximum of 22.0 mm. Moreover, This NiO-CN also decreases the 50% load of *Leishmania donovani* via MTT assay with 25µg/ml concentration after 72 hours incubation.

1. Introduction

In the field of nanotechnology, the incorporation of nanoparticles into composite matrices has had a transformative impact on material science, offering a platform with unprecedented properties and applications. Recently, there has been a growing interest in polymer nanocomposites containing metal nanoparticles, particularly in their unique properties[1-3]. Among the different polymeric matrices available, cellulose stands out as a sustainable organic raw material. Cellulose textiles with a variety of functions can suit the needs of a wide range of applications[4-6]. In particular, the combination of nickel oxide (NiO) nanoparticles with cellulose has attracted significant attention. This amalgamation takes advantage of the distinct attributes of both NiO and cellulose, resulting in a nanocomposite with immense potential in various scientific domains[7-8]. Cellulose is a highly affordable, sustainable, and renewable resource that has garnered considerable attention in recent decades. Researchers have been motivated to develop cellulose-based materials with novel functions[9]. Nanocellulose, which refers to cellulose materials with at least one dimension in the nanometer range, can be isolated from plants or synthesized by bacteria. It exhibits high strength, low density, and high crystallinity, as well as biodegradability and biocompatibility [10]. Metal oxide nanoparticles (MONPs) have attracted considerable interest due to their unique optical, electronic, magnetic, and antibacterial properties[11-13]. Metal oxides like zinc oxide (ZnO), copper oxide (CuO), magnesium oxide (MgO), and

* Corresponding author.
E-mail address anshunadila123@gmail.com (A. Tamta)

doi: 10.5267/j.ccl.2024.2.001

titanium dioxide (TiO_2) have been extensively researched for use in healthcare products, biocides, catalysts, electronics, optical devices, biosensors, and other cutting-edge fields[14-15]. Nanocellulose/metal oxide hybrids with antibacterial, magnetic, sensing, or enhanced absorption capabilities are in high demand for applications such as packaging, wound healing, magnetic resonance imaging (MRI), drug administration, bio-separation, and water purification[16-17]. Metal oxides are chosen in nanocellulose-based antibacterial formulations due to their extended release and lack of microbial resistance, both of which are common with antibiotics[18-19]. The development of microbial resistance is a primary reason for antibiotic failure in treating illnesses. MONPs are efficient against a wide spectrum of bacteria, viruses, and fungi because they produce reactive oxygen species (ROS) that destroy microorganisms [20-21]. ROS attack microorganisms at several places at the same time, causing oxidation and death. There are two methods for making cellulose-based composites[22]. Mechanically incorporating metal nanoparticles into a dissolved cellulose matrix is one way, although this process is hampered by nanoparticle aggregation. It is difficult to reduce nanoparticle aggregation and manage their assemblies at high concentrations[23]. Another strategy is to use interactions between surface-modified cellulose and metal nanoparticles to generate cellulose-based composites in situ. Electrostatic interactions between negatively charged cellulose and positively charged metal ions, for example, can be used to generate cellulose fibers with a high surface coverage of metal nanoparticles[24]. Furthermore, researchers have devised a solution-based approach for converting cotton textiles into conductive textiles by covering cellulose fibers with carbon nanotubes or graphene thin films[25]. This method, however, is ecologically unfavourable due to the usage of organic surfactants in the preparation of the carbon nanotube "ink." The incorporation of NiO nanoparticles into the cellulose matrix confers a variety of functions that show considerable potential in a variety of biological applications[26-27]. Studies have shown that NiO-cellulose nanocomposites (NiO-CN) have biomedical potential, including their use in drug delivery systems, tissue engineering scaffolds, and as antibacterial agents[28]. Furthermore, the synergistic characteristics of NiO and cellulose have demonstrated promising outcomes in environmental remediation procedures such wastewater treatment and pollutant degradation[29].

The present study aims to provide a comprehensive exploration of the synthesis, characterization, and biological activities of NiO-cellulose nanocomposite (NiO-CN). By consolidating the current knowledge in this field, this research seeks to inspire further research efforts and promote the development of innovative and sustainable nanocomposite materials. The main objective of this study is to synthesize NiO-cellulose nanocomposites and evaluate their biological activities, including antibacterial and anti-leishmanial activity.

2. Experimental

2.1 Materials and methods

In this experiment, the precursor of nickel acetate hexahydrate (Merck), along with ethylene glycol (Merck), sodium hydroxide (Merck) and cellulose (Merck) were used. Promastigotes form of *L. donovani* were cultured in M199 medium (Sigma-Aldrich, USA), supplemented with 100 units/mL penicillin (Sigma-Aldrich, USA), 100 µg/mL streptomycin (Sigma-Aldrich, USA) and 10% heat-inactivated fetal bovine serum (FBS; Biowest). We purchased fresh cow milk from a nearby farm in the Almora area. Throughout the studies, a standard solution with known concentration and strength was prepared using double distilled water. Oxalic acid and phenolphthalein were used to standardize NaOH volumetrically. New solutions were utilized during the investigation.

2.2 Synthesis of nickel oxide-cellulose nanocomposite

The initial steps for the synthesis of NiO-CN nanocomposites involved dissolving 0.746 g of nickel acetate in 30 mL of ethylene glycol (a polyol) and constant heating at a temperature of 150° C followed by stirring for 30 min. Now add 4 gm cellulose to the reaction mixture. Now the addition of 60 mL 0.3 N solution of sodium hydroxide solution drops by drop. This 60 mL solution of base was added with a time interval of 10 minutes for each 20 mL with heating and stirring at the same temperature, adding 60 mL of 0.3 N sodium hydroxide solution drop by drop. This 60 mL base solution was added in increments of 10 minutes for each 20 mL, with heating and stirring at the same temperature. Now 10 mL of cow milk was added to the reaction mixture, which was maintained constantly heated and stirred for another hour. The mixture was centrifuged at 2500 rpm for 30 min. The precipitate was collected in a beaker containing an ethyl alcohol and acetone mixture. The precipitate was allowed to settle and the solvent was removed through a decantation process. After the removal of the supernatant liquid, the precipitate of NiO-Cellulose nanocomposite was obtained which was kept in an oven at 150° C for six hours. Finally, grinded with mortar to be shaped into fine particles in powdered form. The sample was maintained in an airtight chamber in a sample tube.

2.2.1 Antibacterial activity

The antibacterial activity of the samples was tested against the selected bacterial strains using agar well diffusion method which was previously reported by Kalemba and Kunicka (2003) with required modifications. The bacteria strains used were *Bacillus subtilis, Salmonela abony, Staphylococcus aureus and Escherichia coli.* Using stock solutions of (100mg/ml) four other concentrations (75mg/ml, 50mg/ml, 25mg/ml, 10mg/ml) of the samples were prepared in the relevant solvent

autoclaved distilled water. Each bacterium was grown in nutrient broth for 24 hours at 37±2 ^{0}C. After 24 hours *Bacillus subtilis, Salmonela abony, Staphylococcus aureus* were evenly spread with the help of sterilized cotton swabs on Nutrient Agar plates while for *Escherichia coli*, MacConkey Agar plates were used for better visualization of zones. Wells were made in each plate with the help of cork borer and samples of different concentrations were placed in each well. The plates were then incubated for another 24 hours at 37±2 ^{0}C[30]. The complete testing was performed under aseptic conditions. The zone of inhibition was calculated using the formula mentioned below:

Zone of Inhibition = (Diameter of the clear zone) - (Diameter of the well)

2.2.2 Antileishmanial activity

L. donovani Bob strain (LdBob strain/MHOM/SD/62/1SCL2D) promastigotes, were cultured in M199 medium (Sigma-Aldrich, USA), supplemented with 100 units/ml penicillin (Sigma-Aldrich, USA), 100 µg/ml streptomycin (Sigma-Aldrich, USA) and 10% heat- inactivated fetal bovine serum (FBS; Biowest). Logarithmic phase *L. donovani* bob strain promastigotes were used to determine the inhibitory efficacy using the MTT assay. The graph of Antileishmanial activity of NiO-CN against Promastigote's form of *L. donovani* has been shown in **Fig.8.** Briefly, parasites were plated on 96-well flat bottom plates at a density of around 10^5 parasites per well with 200µl/well and incubated with different concentrations of NiO-CN for 72 hours. Then 20 µl of MTT (Himedia) stock solution (5 mg/ml) was added to each well of respective plates followed by incubation for 4 hours. Then centrifuged in 1000 g for 15 min, the supernatant was discarded and 100 µL of DMSO was added to each well and resuspended. The O.D. was measured at 570nm by micro-plate reader (Bio Rad). Percentage of inhibition was calculated by comparing the % viability with untreated control. Each experiment was done in triplicates[31-32]. The % viability of cells was calculated by the following formula.

Viability % = (treated cells/untreated cells) ×100

2.2.3 Characterization Techniques

The produced materials were examined using conventional analytical methods such as XRD, TEM, SEM-EDX, FT-IR, and UV-vis spectroscopy. The crystalline nature of produced nanoparticles was determined using an X-Ray Diffractometer (PAN analytical X Pert Pro). The Varian 7000 FTIR Fourier Transform Infrared (FT-IR) spectrometer was used to determine if the functional group was present in the produced material. The surface morphology of the material was investigated using a Zeiss EVO40 scanning electron microscope (SEM). The particle size was measured using a JEOL 2100F Transmission Electron Microscope (TEM). To assess absorbance during anti-inflammatory effect, a UV-visible spectrophotometer (Thermo Scientific, Evolution-201) was utilized.

3. Results and discussions

3.1 XRD Study

Fig.1 and **Table 1** depict the XRD pattern and list of peaks of NiO cellulose nanocomposite (NiO-CN). The X-ray diffraction (XRD) patterns seen in **Fig.1** demonstrate the created NiO cellulose nanocomposite (NiO-CN). The NiO-CN XRD pattern shows significant diffraction peaks at angles of 22.35°, 26.50°, and 34.50°. These peaks reveal essential details regarding the crystalline structure of NiO-CN. Previously, various studies showed cellulose XRD peaks around 22.4° and 22.6°, which are virtually identical to our XRD results[33-34]. It has been also reported in previous studies that the shape of NiO nanoparticles was demonstrated by the characteristics peak at 26.98[35] and 34.50°[36-37] which also resembled our present study.

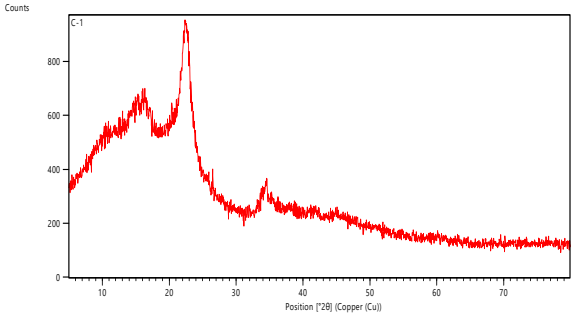

Fig. 1. XRD patterns of NiO cellulose nanocomposite (NiO-CN)

Table 1. List of peak of XRD patterns of NiO cellulose nanocomposite (NiO-CN)

Sl. No	Pos. [°2θ]	FWHM Total [°2θ]	d-spacing [Å]	Rel. Int. [%]	Area [cps*°2θ]
1.	22.3520	0.1761	3.97423	88.93	2.39
2.	26.5091	0.0660	3.35968	65.74	0.33
3.	34.5054	0.7178	2.59721	100.00	10.97

3.2 TEM Study

Fig. 2(a-b) shows a TEM image of NiO cellulose nanocomposite (NiO-CN). The average crystallite size TEM data improves particle size measurements and boosts nanomaterial characteristics. The particle size of the produced nanoparticles is shown by TEM to be in the region of 20-30 nm.

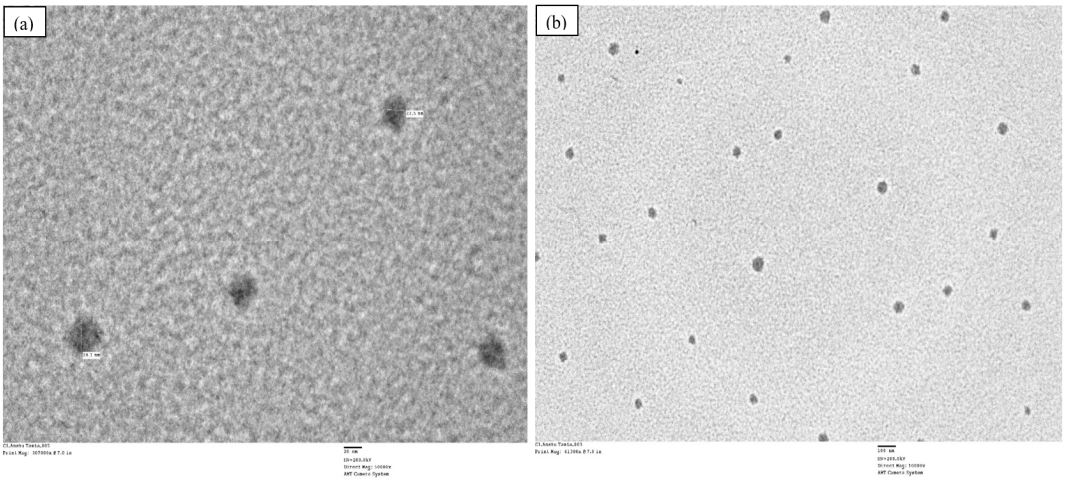

Fig. 2(a, b) TEM image of NiO cellulose nanocomposite (NiO-CN)

3.3 SEM Analysis

The surface morphology of NiO-cellulose nanocomposite (NiO-CN) was studied using scanning electron microscopy (SEM). The morphology of the NiO-CN is depicted in **Fig. 3(a-f)**. The images show that the particles are highly agglomerated. As a result of this aggregation or overlap of smaller particles, some larger particles are detected. The images show NiO-CN aggregates formed by self-assembled fractal architectures caused by the presence of strong hydrogen bonds. These interactions are promoted by the hydroxyl groups on the surface of the cellulose fibrils and are greatly dependent on the cellulose source and extraction procedure[38].

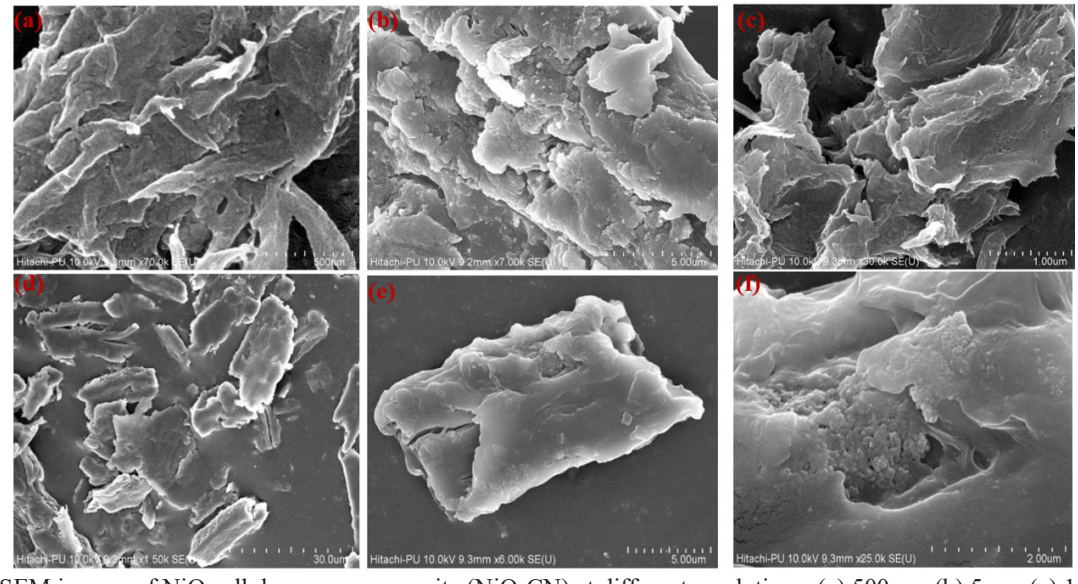

Fig. 3. SEM images of NiO cellulose nanocomposite (NiO-CN) at different resolutions: (a) 500 nm (b) 5 µm (c) 1 µm, (d) 30 nm, (e) 5 nm, (f) 2µm

3.4 EDX Study

Fig. 4 depicts the EDX spectrum of NiO cellulose nanocomposite (NiO-CN), which revealed that the weight percentages of C, O, Ni, and N-elements in the synthesized material were 41.65%, 52.49%, 3.81%, and 2.06%, respectively.

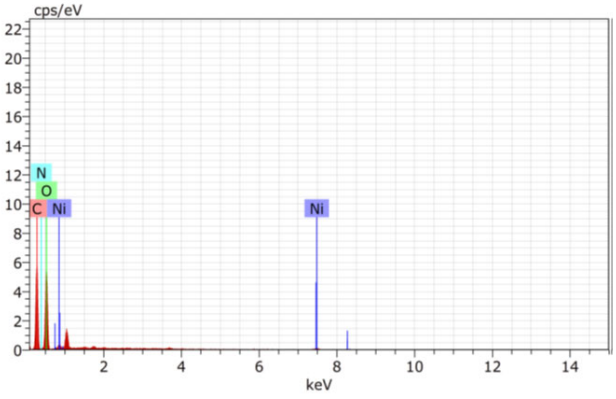

Spectrum: test 17181

Element	Series	unn. C [wt.%]	norm. C [wt.%]	Atom. C [at.%]	Error (3 Sigma) [wt.%]
Carbon	K-series	41.65	41.65	49.82	17.47
Oxygen	K-series	52.49	52.49	47.13	21.89
Nickel	K-series	3.81	3.81	0.93	0.79
Nitrogen	K-series	2.06	2.06	2.11	2.73
Total:		100.00	100.00	100.00	

Fig. 4. EDX spectra of NiO cellulose nanocomposite (NiO-CN)

3.5 FT-IR Study

The FTIR spectra of NiO cellulose nanocomposite (NiO-CN) are shown in **Fig. 5.** Significant peaks in this spectrum may be seen at 611 cm^{-1}, 665 cm^{-1}, 1059 cm^{-1}, 1109 cm^{-1}, 1159 cm^{-1}, 1235 cm^{-1}, 1380 cm^{-1}, 1420 cm^{-1}, 1598 cm^{-1}, 2135 cm^{-1}, 2918 cm^{-1}, and 3402 cm^{-1}. The O-H stretching vibration mode is given to the strong band at 3430 cm^{-1} [39]. At 1059 cm^{-1}, the strong bond corresponds to the Ni-O stretching vibration mode of Ni-O[36]. The presence of peaks of 2853 cm^{-1}, 2922 cm^{-1} and 3431 cm^{-1} are characteristics of the hydroxyl group (O-H) stretching the adsorbed water molecule[40]. The strong bond corresponds to the Ni-O stretching vibration mode of Ni-O at 1081 cm^{-1} [36]. In the second region, the band at 1439 cm^{-1} is assigned to O-H bending due to the presence of a carboxylic group in precursors. Similarly, the peak at 1571 cm^{-1} can be assigned due to the interaction of nanoparticles with cow milk as a capping reagent or as adsorbed molecule at the surface of the nanoparticle[41]. It has been reported that the presence of peaks at 1543 cm^{-1} and 1474 cm^{-1} also shows the presence of triazine rings, which confirms the presence of melamine in the Cellulose nanocrystals (CNC) construction. Further, the extending vibration C-O-C related to the pyranose ring was apparent at bands 1019 cm^{-1} and 1060 $cm^{-1}$and CH vibrations at 897 cm^{-1}, which are available in both microcrystalline cellulose (MCC) and Cellulose nanocrystals (CNCs)[42]. The spectra show that the peaks at 1380 cm^{-1} were displayed according to the bending vibrations of N-H that blue shifted to 611 cm^{-1}, which indicated the presence of NiO nanoparticles[43].

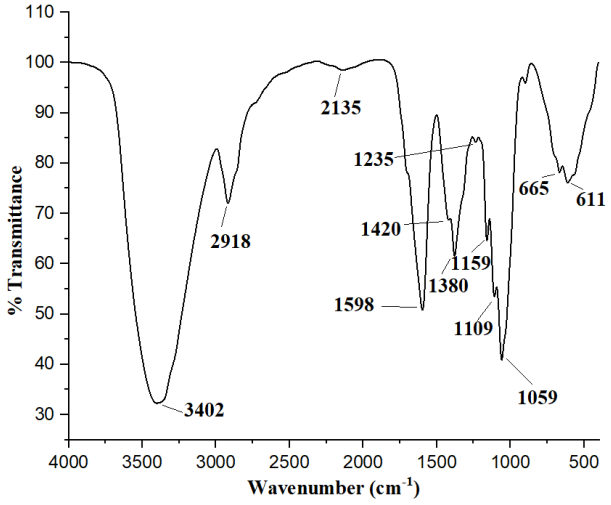

Fig. 5. FTIR spectrum of NiO cellulose nanocomposite (NiO-CN)

3.6 UV-Vis study

UV-vis absorption spectra were obtained at increasing temperatures to study the optical properties of the produced NiO cellulose nanocomposite (NiO-CN), as shown in **Fig. 6.** The UV-vis spectroscopy indicates an absorption peak at 353 nm, and the band gap energy of these nanoparticles is calculated using the Tauc-equation:

$$\alpha h\nu = A(h\nu - Eg)^n \quad (2)$$

where α is the absorption coefficient, h is the photon energy, and Eg is the band-gap for direct transitions (n=2). In the inset of **Fig. 6**, a plot of $(\alpha h\upsilon)^2$ ($eV^2.cm^{-2}$) versus hν (eV) is displayed, and the linear component of the curve is projected to the hυ axis to calculate the band gap. The band gap was discovered to be 1.8 eV.

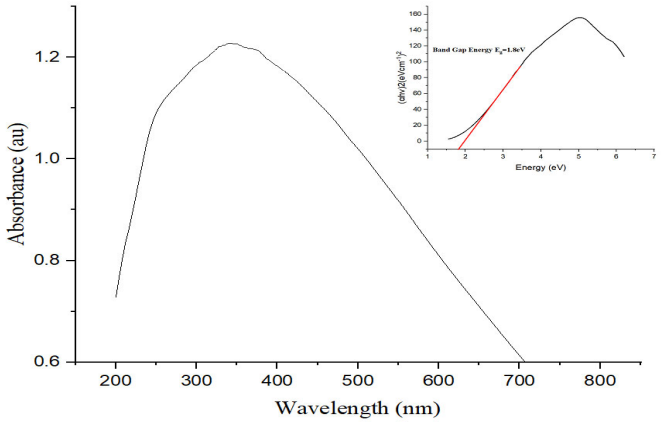

Fig. 6. UV–vis spectrum and Tauc-plot (insert) of NiO cellulose nanocomposite (NiO-CN)

3.7 Antibacterial activity

The results indicated that NiO cellulose nanocomposite (NiO-CN) inhibited the growth of all the selected bacteria. The inhibition was dose dependent i.e., the concentration of 100mg/ml showed the maximum inhibition followed by 75mg/ml and so on. The maximum inhibition was found in the bacterium *Bacillus subtilis,* where clear zones of 22mm, 19mm, 13mm, 12mm, and 9mm were observed for the concentrations of 100mg/ml, 75mg/ml, 50mg/ml, 25mg/ml and 10mg/ml respectively. Following *B. subtilis,* maximum inhibition was seen in *S. abony*, at the similar pattern where maximum inhibition was found at 100mg/ml and least in 10mg/ml. The zone of inhibition was found to be 17mm, 12mm, 9mm, 7.5mm, 4mm in order of decreasing concentrations. For *S. aureus,* the zone of inhibition was found out be 15mm, 13.5mm, 12mm, 10mm, and 3mm in decreasing order of concentrations. The least inhibition by NiO cellulose nanocomposite (NiO-CN) was found to be in *E. coli,* where zone of inhibition was found to 8mm, 7mm, 5mm, 3mm and 3mm for the conc. of 100mg/ml,75mg/ml, 50mg/ml, 25mg/ml, and 10mg/ml respectively.

Table 2. The antibacterial activity of NiO cellulose nanocomposite (NiO-CN) at different concentrations

Sl. No	NiO-CN	10mg/ml	25mg/ml	50mg/ml	75mg/ml	100mg/ml
1.	*B. subtilis*	9mm	12mm	13mm	19mm	22mm
2.	*S. abony*	4mm	7.5mm	9mm	12mm	17mm
3.	*S. aureus*	3mm	10mm	12mm	13.5mm	15mm
4.	*E. coli*	3mm	3mm	5mm	7mm	8mm

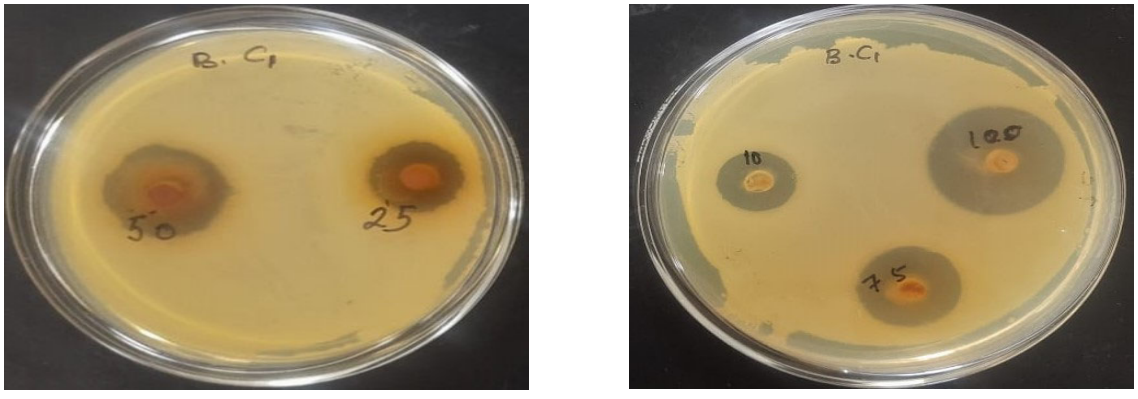

[a] B. Subtillis

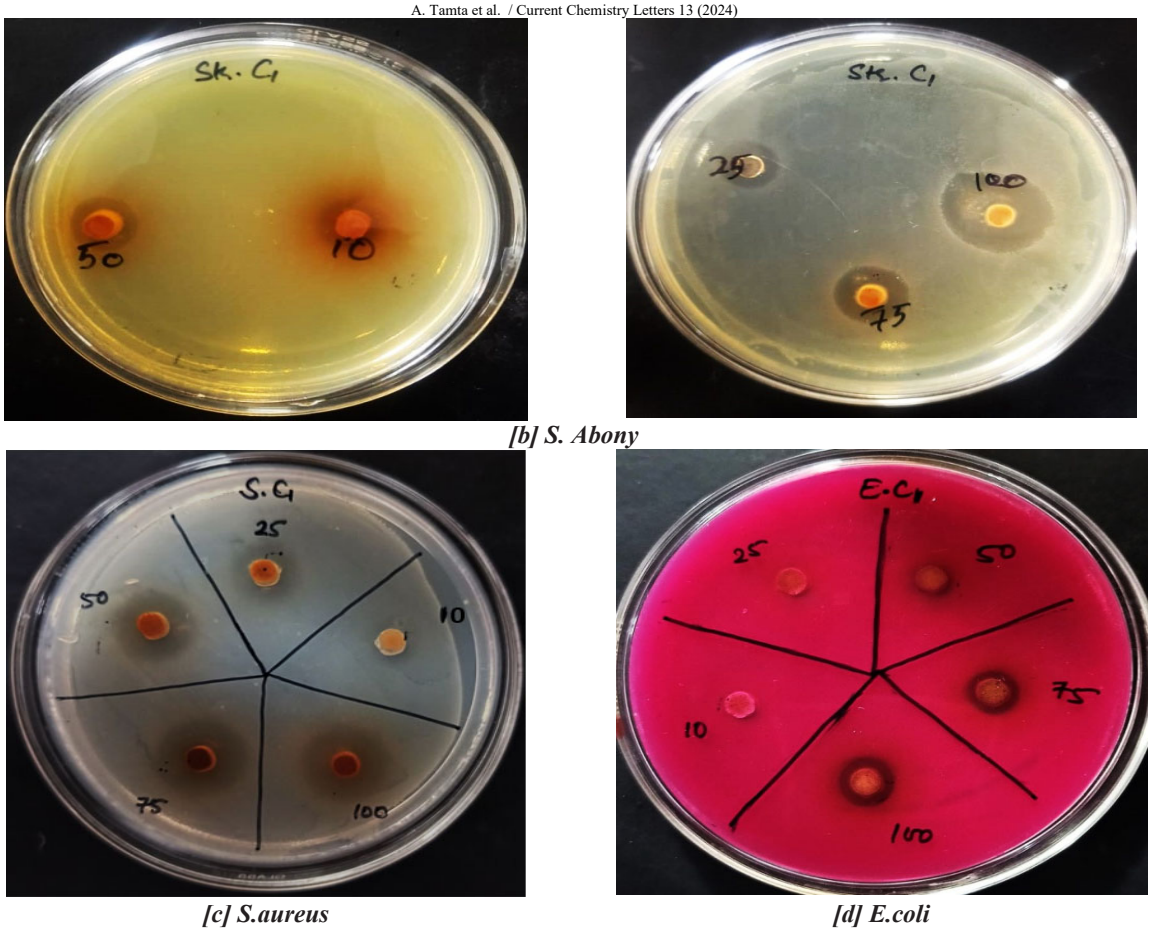

Fig. 7. Antibacterial of NiO cellulose nanocomposite [a] *B. subtilis,* [b] *S. Abony* [c] *Staphylococcus aureus* and [d] *E. coli*

3.8 Antileishmanial activity

Antileishmanial activity of the NiO cellulose nanocomposite (NiO-CN) was studied with doses ranging from 0 to 1000µg/mL on the promastigote form of *L. donovani*. The viability of promastigotes was determined by MTT assay. The conversion of tetrazolium salt to an insoluble formazan product by the mitochondrial electron transport chain is an indicator of promastigote viability while a decrease in the amount of formazan indicates toxicity to the *Leishmania*. At zero concentration, untreated cells were shown healthy and moving but after the treatment of NiO-CN *Leishmania* cells went towards death. 50% cell viability of *Leishmania* exhibited at 25µg/ml concentration after 72 hours incubation. Up to 1000 µg/ml concentration, only 25% leishmanial cells survived. According to the potential activity of NiO-CN against the promastigote form of *Leishmania donovani* may be evaluated as a successful agent against antileishmanial activity and help to develop an alternative option for the treatment of visceral Leishmaniasis.

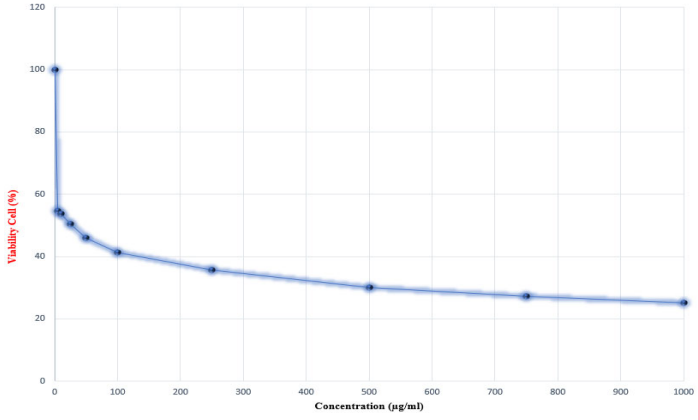

Fig. 8. Antileishmanial activity of NiO-CN against Promastigotes form of *L. donovani*

4. Conclusions

The synthesis of NiO cellulose nanocomposite (NiO-CN) using milk at a higher concentration and reducing ethylene glycol concentration offers a greener, more sustainable method for producing NiO cellulose nanocomposite (NiO-CN). This study is a primary step toward green chemistry in synthesis NiO-CN, paving the way for further research in green chemistry. NiO cellulose nanocomposite (NiO-CN) have demonstrated significant biological activities, including antibacterial and antileishmanial. These diverse activities make them promising candidates for a range of biomedical applications. The antibacterial activity of NiO cellulose nanocomposite (NiO-CN) against *Bacillus subtilis* and *Staphylococcus aureus Salmonela abony,* and *Escherichia coli* highlights their potential in combating bacterial infections. Furthermore, Due to lack of effective vaccines visceral leishmaniasis is lethal in various ways if remain untreated. Now, alternative options are required against this disease. NiO-CN showed antileishmanial activity against *Leishmania* parasites (*Leishmania donovani*) provides a new avenue for the treatment of visceral leishmaniasis.

Acknowledgement

The authors acknowledge the Malaviya National Institute of Technology Jaipur, Jawaharlal Nehru University, New Delhi-110067 and ICAR-VPKAS Almora, Uttarakhand India, for providing the instrumentational facilities. The authors are thankful to Prof. Raj N. Mehrotra Former Professor and Head Department of Chemistry, at Jodhpur University for useful and valuable suggestions.

References

1. Ghazzy, A., Naik, R.R. and Shakya, A.K. **(2023)** Metal–Polymer Nanocomposites: A Promising Approach to Antibacterial Materials. *Polymers*, *15*(9), 2167.
2. Jancar, J., Douglas, J.F., Starr, F.W., Kumar, S.K., Cassagnau, P., Lesser, A.J., Sternstein, S.S. and Buehler, M.J. **(2010)** Current issues in research on structure–property relationships in polymer nanocomposites. *Polymer*, *51*(15), 3321-3343.
3. Faupel, F., Zaporojtchenko, V., Strunskus, T. and Elbahri, M. **(2010)** Metal-polymer nanocomposites for functional applications. *Advanced engineering materials*, *12*(12), 1177-1190.
4. Rashid, A.B., Hoque, M.E., Kabir, N., Rifat, F.F., Ishrak, H., Alqahtani, A. and Chowdhury, M.E. **(2023)** Synthesis, Properties, Applications, and Future Prospective of Cellulose Nanocrystals. *Polymers*, *15*(20), 4070.
5. Gabrielli, V. and Frasconi, M. **(2022)** Cellulose-based functional materials for sensing. *Chemosensors*, *10*(9), 352.
6. Bej, S., Sarma, H., Ghosh, M. and Banerjee, P. **(2023)** Metal-organic-frameworks/cellulose hybrids with their modern technological implementation towards water treatment. *Environmental Pollution*, 121278.
7. Karimzadeh, Z., Mahmoudpour, M., Rahimpour, E. and Jouyban, A. **(2022)** Nanomaterial based PVA nanocomposite hydrogels for biomedical sensing: Advances toward designing the ideal flexible/wearable nanoprobes. *Advances in Colloid and Interface Science*, *305*, 102705.
8. Shi, C., Kang, F., Zhu, Y., Teng, M., Shi, J., Qi, H., Huang, Z., Si, C., Jiang, F. and Hu, J. **(2023)** Photoreforming lignocellulosic biomass for hydrogen production: Optimized design of photocatalyst and photocatalytic system. *Chemical Engineering Journal*, *452*, 138980.
9. Aziz, T., Farid, A., Haq, F., Kiran, M., Ullah, A., Zhang, K., Li, C., Ghazanfar, S., Sun, H., Ullah, R. and Ali, A. **(2022)** A review on the modification of cellulose and its applications. *Polymers*, *14*(15), 3206.
10. Barhoum, A., Rastogi, V.K., Mahur, B.K., Rastogi, A., Abdel-Haleem, F.M. and Samyn, P. **(2022)** Nanocelluloses as new generation materials: Natural resources, structure-related properties, engineering nanostructures, and technical challenges. *Materials Today Chemistry*, *26*, 101247.
11. Pathak, J., Pandey, B., Singh, P., Kumar, R., Kaushik, S., Sahu, I.P., Thakur, T.K. and Kumar, A. **(2023)** Exploring the paradigm of phyto-nanofabricated metal oxide nanoparticles: recent advancements, applications, and challenges. *Molecular Biotechnology*, 1-21.
12. Joshi, N., Pandey, D.K., Mistry, B.G. and Singh, D.K. **(2023)** Metal Oxide Nanoparticles: Synthesis, Properties, Characterization, and Applications. In *Nanomaterials: Advances and Applications*, 103-144.
13. Khan, A., Vishvakarma, R., Sharma, P., Sharma, S. and Vimal, A. **(2023)** Green Synthesis of Metal-Oxide Nanoparticles from Fruits and Their Waste Materials for Diverse Applications. In *Nanomaterials from Agricultural and Horticultural Products*, 81-119.
14. Salem, S.S., Hammad, E.N., Mohamed, A.A. and El-Dougdoug, W. **(2022)** A comprehensive review of nanomaterials: Types, synthesis, characterization, and applications. *Biointerface Res. Appl. Chem*, *13*(1), 41.
15. Yadav, V.K., Khan, S.H., Malik, P., Thappa, A., Suriyaprabha, R., Ravi, R.K., Choudhary, N., Kalasariya, H. and Gnanamoorthy, G. **(2020)** Microbial synthesis of nanoparticles and their applications for wastewater treatment. *Microbial Biotechnology: Basic Research and Applications*, 147-187.
16. Oprea, M. and Panaitescu, D.M. **(2020)** Nanocellulose hybrids with metal oxides nanoparticles for biomedical applications. *Molecules*, *25*(18), 4045.
17. Oun, A.A., Shankar, S. and Rhim, J.W. **(2020)** Multifunctional nanocellulose/metal and metal oxide nanoparticle hybrid nanomaterials. *Critical reviews in food science and nutrition*, *60*(3), 435-460.

18. Oprea, M. and Panaitescu, D.M. **(2020)** Nanocellulose hybrids with metal oxides nanoparticles for biomedical applications. *Molecules*, *25*(18), 4045.
19. Thomas, B., Raj, M.C., Joy, J., Moores, A., Drisko, G.L. and Sanchez, C. **(2018)** Nanocellulose, a versatile green platform: from biosources to materials and their applications. *Chemical reviews*, *118*(24), 11575-11625.
20. Abo-zeid, Y. and Williams, G.R. **(2020)** The potential anti-infective applications of metal oxide nanoparticles: A systematic review. *Wiley Interdisciplinary Reviews: Nanomedicine and Nanobiotechnology*, *12*(2), 1592.
21. Kaur, H., Rauwel, P. and Rauwel, E. **(2023)** Antimicrobial nanoparticles: synthesis, mechanism of actions. In *Antimicrobial activity of nanoparticles*, 155-202.
22. Abdelhamid, H.N. and Mathew, A.P. **(2022)** Cellulose-based nanomaterials advance biomedicine: a review. *International Journal of Molecular Sciences*, *23*(10), 5405.
23. Thoniyot, P., Tan, M.J., Karim, A.A., Young, D.J. and Loh, X.J. **(2015)** Nanoparticle–hydrogel composites: Concept, design, and applications of these promising, multi-functional materials. *Advanced Science*, *2*(1-2), 1400010.
24. Rol, F., Belgacem, M.N., Gandini, A. and Bras, J. **(2019)** Recent advances in surface-modified cellulose nanofibrils. *Progress in Polymer Science*, *88*, 241-264.
25. Zhao, D., Zhu, Y., Cheng, W., Chen, W., Wu, Y. and Yu, H. **(2021)** Cellulose-based flexible functional materials for emerging intelligent electronics. *Advanced materials*, *33*(28), 2000619.
26. Shen, Y. **(2015)** Carbothermal synthesis of metal-functionalized nanostructures for energy and environmental applications. *Journal of Materials Chemistry A*, *3*(25), 13114-13188.
27. Ziegler, J.M., Andoni, I., Choi, E.J., Fang, L., Flores-Zuleta, H., Humphrey, N.J., Kim, D.H., Shin, J., Youn, H. and Penner, R.M. **(2020)** Sensors based upon nanowires, nanotubes, and nanoribbons: 2016–2020. *Analytical Chemistry*, *93*(1), 124-166.
28. Joseph, B., Sagarika, V.K., Sabu, C., Kalarikkal, N. and Thomas, S. **(2020)** Cellulose nanocomposites: Fabrication and biomedical applications. *Journal of Bioresources and Bioproducts*, *5*(4), 223-237.
29. Maksoud, M.A., Elgarahy, A.M., Farrell, C., Ala'a, H., Rooney, D.W. and Osman, A.I. **(2020)** Insight on water remediation application using magnetic nanomaterials and biosorbents. *Coordination Chemistry Reviews*, *403*, 213096.
30. Zaidan, M. R., Noor Rain, A., Badrul, A. R., Adlin, A., Norazah, A., Zakiah, I. **(2005)** In vitro screening of five local medicinal plants for antibacterial activity using disc diffusion method. *Trop biomed*, *22*(2), 165-170.
31. Tandon, S., Puri, M., Bharath, Y., Choudhury, U. M., Mohapatra, D. K., Muthuswami, R., Madhubala, R. **(2023)** In vitro screening of natural product-based compounds for leishmanicidal activity. *Journal of Parasitic Diseases*, 1-15.
32. Prasanna, P., Kumar, P., Mandal, S., Kumar, S., Payal, T., Sk, U. H., Mandal, D. **(2021)** Synthesis of 7, 8–dihydroxyflavone functionalized gold nanoparticles and its mechanism of action against Leishmania donovani.
33. Gong, J., Li, J., Xu, J., Xiang, Z. and Mo, L. **(2017)** Research on cellulose nanocrystals produced from cellulose sources with various polymorphs. *RSC advances*, *7*(53), 33486-33493.
34. El-Sheekh, M.M., Yousuf, W.E., Kenawy, E.R. and Mohamed, T.M. **(2023)** Biosynthesis of cellulose from Ulva lactuca, manufacture of nanocellulose and its application as antimicrobial polymer. *Scientific Reports*, *13*(1), 10188.
35. Abbasi, B.A., Iqbal, J., Yaseen, T., Zahra, S.A., Ali, S., Uddin, S., Mahmood, T., Kanwal, S., El-Serehy, H.A., and Chalgham, W. **(2023)** Exploring Physical Characterization and Different Bio-Applications of Elaeagnus angustifolia Orchestrated Nickel Oxide Nanoparticles. *Molecules*, *28*(2), 654.
36. Sankar, A. U. R., Kiran, Y. B., Mohan, V. M., Kumar, A. K., and Varalakshmi, M. V. **(2023)** Green synthesis of cotton flower shaped nickel oxide nanoparticles: Anti-bacterial and tribological studies. *Inorganic Chemistry Communications*, *157*, 111239.
37. Habtemariam, A. B., Oumer, M. **(2020)** Plant extract mediated synthesis of nickel oxide nanoparticles. *Mater. Int*, *2*, 205-209.
38. Habibi, Y., Lucia, L. A. and Rojas, O. J. **(2010)** Cellulose nanocrystals: chemistry, self-assembly, and applications. *Chemical reviews*, *110*(6), 3479-3500.
39. G. T. Anand, R. Nithiyavathi, R. Ramesh, S. J. Sundaram and K. Kaviyarasu. **,2020)** Structural and optical properties of nickel oxide nanoparticles: investigation of antimicrobial applications. *Surf. Interfaces,* 18, 100460.
40. S. T. Fardood, A. Ramazani and S. Moradi. **(2017)** A novel green synthesis of nickel oxide nanoparticles using Arabic gum". *ChemJMold.* 12, 115-118.
41. S. M. Gholami, S. Z. Gholami, G. M. Shams, A. Akbarzadeh, G. Riazi and A. M. Razzaghi. **(2016)** Biogenic approach using sheep milk for the synthesis of platinum nanoparticles: the role of milk protein in platinum reduction and stabilization". *Int. J. Nanosci. Nanotechnol.* 12, 199-206.
42. Deepa, B., Abraham, E., Cordeiro, N., Mozetic, M., Mathew, A. P., Oksman, K., Pothan, L. A. **(2015)** Utilization of various lignocellulosic biomass for the production of nanocellulose: a comparative study. *Cellulose*, *22*, 1075-1090.
43. Abd El-Lateef, H. M., Gouda, M. **(2021)** Novel nanocomposites of nickel and copper oxide nanoparticles embedded in a melamine framework containing cellulose nanocrystals: Material features and corrosion protection applications. *Journal of Molecular Liquids*, *342*, 116960.